J. Phys. A: Math. Gen. 25 (1992) 4127–4137. Printed in the UK

Non-algebraic domain growth in binary alloys with quenched disorder

Sanjay Puri†‡ and Nita Parekh†

† School of Physical Sciences, Jawaharlal Nehru University, New Delhi 110067, India
‡ Institut für Physik, Johannes-Gutenberg Universität Mainz, 6500 Mainz 1, Federal Republic of Germany

Received 24 January 1992

Abstract. We present detailed numerical results from a computationally efficient cell dynamical system (CDS) model of domain growth in binary alloys with quenched disorder. Our numerical results suggest that the domain growth law for the disordered case is compatible with $\langle R\rangle(t) \sim (\ln t)^x$, where x has a weak dependence on the disorder amplitude. However, it is possible that our simulations do not access the true asymptotic regime. We also find that the scaled structure factor for the disordered case is independent of the amplitude of disorder and is the same as that for the pure system.

1. Introduction

Much recent attention has focused on the dynamics of phase ordering, namely, the mechanisms whereby a binary system, rendered thermodynamically unstable by quenching, orders into distinct phases [1]. It is now well established that, for pure systems, the ordering process is characterized by a unique length scale $R(t)$ (where t is the time). This length scale shows a power-law growth in time, i.e. $R(t) \sim t^{\phi}$, where ϕ is referred to as the growth exponent. For the case of a non-conserved order parameter (e.g. ordering of a ferromagnet), it is known that $\phi = \frac{1}{2}$. This result has been established experimentally, numerically and theoretically [1]. For the case of a conserved order parameter without hydrodynamic effects (e.g. segregation of a binary alloy), we know that $\phi = \frac{1}{3}$ [1]. This result was experimentally known and theoretically expected for some time. However, it was well established numerically only after the advent of computationally efficient cell dynamical system (CDS) models [2]. Finally, for the case of a conserved order parameter with hydrodynamic effects (e.g. segregation of a binary fluid), it has been experimentally and theoretically believed that $\phi = 1$ [1]. Numerically, this has only been demonstrated very recently [3], again with the use of CDS models.

Domain growth laws in the case of a conserved order parameter have been the cause of a fair amount of numerical controversy and much effort has been devoted to conclusively establish the above results. As a consequence, less attention has been paid to more realistic situations, e.g. phase ordering dynamics in systems with quenched or annealed disorder [4]. In an attempt to understand the role played by quenched disorder in affecting the dynamics of phase ordering, we have initiated an investigation of CDS models with disorder [5]. Our experience shows that coarse-grained models have been considerably more successful numerically than microscopic models in elucidating the nature of domain growth in pure systems. However, to the best of our

0305-4470/92/154127+11$04.50

knowledge, all previous numerical studies of domain growth in disordered systems have used microscopic models with Monte Carlo dynamics [4]. We believe that our coarse-grained models will be useful in extracting the asymptotic behaviour of domain growth in systems with quenched disorder. In a previous letter [5] we reported numerical results for the case of a non-conserved CDS model with quenched disorder, which is expected to mimic domain growth in a random exchange Ising magnet. In this paper we elaborate on our modelling and report detailed numerical results for the case of a disordered CDS model with conserved order parameter, which is expected to mimic a binary alloy with quenched disorder (e.g. immobile vacancies).

This paper is organized as follows. In section 2, we describe our CDS models and briefly summarize the numerical results obtained for the non-conserved case [5]. In section 3, we describe our results for the case of the conserved order parameter. In section 4, we end with a summary and discussion.

2. Cell dynamical system models with disorder

The starting point of our modelling is the time-dependent Ginzburg-Landau (TDGL) equation, which describes the temporal evolution of a system described by a non-conserved order parameter (e.g. a coarse-grained version of the Ising model with Glauber kinetics [7])

$$\frac{\partial\psi(\boldsymbol{r},t)}{\partial t}=-L\frac{\delta H[\psi(\boldsymbol{r},t)]}{\delta\psi(\boldsymbol{r},t)}+\sigma(\boldsymbol{r},t). \tag{2.1}$$

In (2.1), $\psi(\boldsymbol{r},t)$ is the scalar order parameter at point $\boldsymbol{r}$ and time t; and L is a phenomenological parameter. For the pure Ising model, the coarse-grained free-energy functional $H[\psi(\boldsymbol{r},t)]$ in (2.1) is usually taken to be of the ϕ^4 form

$$H[\psi(\boldsymbol{r},t)]=\int \mathrm{d}\boldsymbol{r}\left[-\frac{\tau}{2}\psi(\boldsymbol{r},t)^2+\frac{g}{4}\psi(\boldsymbol{r},t)^4+\frac{K}{2}(\nabla\psi(\boldsymbol{r},t))^2\right] \tag{2.2}$$

where τ, g and K are phenomenological constants which respectively measure the temperature T ($\tau\sim(T_c-T)$, where T_c is the critical temperature); the coupling constant; and the interfacial energy. The Gaussian white noise $\sigma(\boldsymbol{r},t)$ satisfies the fluctuation-dissipation relation

$$\langle\sigma(\boldsymbol{r},t)\sigma(\boldsymbol{r}',t')\rangle=2TL\delta(\boldsymbol{r}-\boldsymbol{r}')\delta(t-t') \tag{2.3}$$

where we have taken the Boltzmann constant to be unity. The TDGL equation corresponding to the free-energy functional (2.2) (usually referred to as model A [8]) is then

$$\frac{\partial\psi(\boldsymbol{r},t)}{\partial t}=L[\tau\psi(\boldsymbol{r},t)-g\psi(\boldsymbol{r},t)^3+K\nabla^2\psi(\boldsymbol{r},t)]+\sigma(\boldsymbol{r},t). \tag{2.4}$$

For the case of the Ising model with quenched impurities (e.g. site dilution or randomization of exchange interactions), the coarse-grained free-energy functional is usually taken to be of the form [9]

$$H[\psi(\boldsymbol{r},t)]=\int \mathrm{d}\boldsymbol{r}\left[-\frac{\tau(\boldsymbol{r})}{2}\psi(\boldsymbol{r},t)^2+\frac{g(\boldsymbol{r})}{4}\psi(\boldsymbol{r},t)^4+\frac{K(\boldsymbol{r})}{2}(\nabla\psi(\boldsymbol{r},t))^2\right] \tag{2.5}$$

so that the phenomenological measures of the various parameters assume a spatial dependence. The spatial dependence is of the form of a random Gaussian fluctuation

about a constant average, e.g. $\tau(\boldsymbol{r}) = \tau_0 + \delta\tau(\boldsymbol{r})$, $g(\boldsymbol{r}) = g_0 + \delta g(\boldsymbol{r})$ and so on. Then, the TDGL equation corresponding to (2.5) describes the dynamics of the coarse-grained version of the random exchange Ising model (REIM). (This conclusion is supported by a derivation of the coarse-grained kinetic equation by applying the master equation approach [7] to the REIM [10].) For simplicity, we confine ourselves to the case where the interfacial energy is not spatially varying, i.e. $K(\boldsymbol{r}) \equiv K$. This restriction only affects the precise form of the interface between domains and does not change asymptotic results, which are independent of the precise form of the interface. Thus, we consider the TDGL equation

$$\frac{\partial\psi(\boldsymbol{r}, t)}{\partial t} = L[\tau(\boldsymbol{r})\psi(\boldsymbol{r}, t) - g(\boldsymbol{r})\psi(\boldsymbol{r}, t)^3 + K\nabla^2\psi(\boldsymbol{r}, t)] + \sigma(\boldsymbol{r}, t). \tag{2.6}$$

The corresponding partial differential equation for the temporal evolution of a binary alloy with quenched disorder (e.g. immobile vacancies) is

$$\frac{\partial\psi(\boldsymbol{r}, t)}{\partial t} = -L\nabla^2[\tau(\boldsymbol{r})\psi(\boldsymbol{r}, t) - g(\boldsymbol{r})\psi(\boldsymbol{r}, t)^3 + K\nabla^2\psi(\boldsymbol{r}, t)] + f(\boldsymbol{r}, t). \tag{2.7}$$

Equation (2.7) is a generalization of the Cahn-Hillard-Cook equation [11], which describes the evolution of a pure binary alloy undergoing phase segregation. This phenomenological equation can be motivated [10] by applying the master equation approach [7] to the REIM with Kawasaki kinetics, which is the appropriate microscopic model for this case. In (2.7), the noise $f(\boldsymbol{r}, t)$ is Gaussian with mean zero and satisfies the fluctuation-dissipation relation

$$\langle f(\boldsymbol{r}, t) f(\boldsymbol{r}', t')\rangle = -2TL\nabla^2\delta(\boldsymbol{r} - \boldsymbol{r}')\delta(t - t'). \tag{2.8}$$

We next rescale (2.7) and cast it in a dimensionless form, which is more convenient to deal with. We rescale as follows:

$$\begin{aligned} \psi &= \sqrt{\frac{\tau_0}{g_0}}\,\psi' \\ \boldsymbol{r} &= \sqrt{\frac{K}{\tau_0}}\,\boldsymbol{r}' \\ t &= \frac{K}{L\tau_0^2}\,t' \\ f(\boldsymbol{r}, t) &= \frac{L\tau_0}{K}\sqrt{2T\tau_0\left(\frac{\tau_0}{K}\right)^{d/2}}\,\theta(\boldsymbol{r}, t). \end{aligned} \tag{2.9}$$

The corresponding dimensionless form of (2.7) is (dropping the primes)

$$\frac{\partial\psi(\boldsymbol{r}, t)}{\partial t} = -\nabla^2[(1 + \delta a(\boldsymbol{r}))\psi(\boldsymbol{r}, t) - (1 + \delta b(\boldsymbol{r}))\psi(\boldsymbol{r}, t)^3 + \nabla^2\psi(\boldsymbol{r}, t)] + \sqrt{\varepsilon}\,\theta(\boldsymbol{r}, t) \tag{2.10}$$

where $\delta a(\boldsymbol{r}) = \delta\tau(\boldsymbol{r})/\tau_0$ and $\delta b(\boldsymbol{r}) = \delta g(\boldsymbol{r})/g_0$ are random Gaussian fluctuations about zero. In (2.10)

$$\varepsilon = \frac{2g_0 T}{\tau_0^2}\left(\frac{\tau_0}{K}\right)^{d/2} \tag{2.11}$$

and $\theta(\boldsymbol{r}, t)$ is a Gaussian white noise which satisfies

$$\langle\theta(\boldsymbol{r}, t)\theta(\boldsymbol{r}', t')\rangle = -\nabla^2\delta(\boldsymbol{r} - \boldsymbol{r}')\delta(t - t'). \tag{2.12}$$

In [5] we proposed a computationally efficient CDS model which mimics the dynamics of (2.6). The prescription for obtaining such models for reaction-diffusion equations has been extensively discussed in the literature [2] and we do not repeat it here. Briefly, the basic idea of this modelling is to directly integrate the deterministic local part (i.e., the 'reaction' part) of the reaction-diffusion equation. This solution is then used to construct a new numerical scheme for the reaction-diffusion equation. The major advantage of this new scheme is that it enables the use of rather coarse mesh sizes to simulate the partial differential equation [12]. We do not go into further details of the procedure here. Rather, we directly write down the CDS model that mimics the dynamics of the appropriate dimensionless form of (2.6) [2]

$$\psi(\boldsymbol{r}, t+\Delta t)=\frac{\alpha(\boldsymbol{r})A(\boldsymbol{r})\psi(\boldsymbol{r}, t)}{\sqrt{\alpha(\boldsymbol{r})^2+\psi(\boldsymbol{r}, t)^2(A(\boldsymbol{r})^2-1)}}+\frac{\Delta t}{(\Delta x)^2}\Delta_D\psi(\boldsymbol{r}, t)+\sqrt{\varepsilon}\Delta t\mu(\boldsymbol{r}, t)$$

$$=G_r(\psi(\boldsymbol{r}, t))+\frac{\Delta t}{(\Delta x)^2}\Delta_D\psi(\boldsymbol{r}, t)+\sqrt{\varepsilon}\Delta t\mu(\boldsymbol{r}, t) \tag{2.13}$$

where Δt and Δx are the mesh sizes in time and space respectively; and

$$\alpha(\boldsymbol{r})=\sqrt{\frac{1+\delta a(\boldsymbol{r})}{1+\delta b(\boldsymbol{r})}}$$
$$A(\boldsymbol{r})=\mathrm{e}^{(1+\delta a(\boldsymbol{r}))\Delta t}. \tag{2.14}$$

In (2.13), Δ_D is the isotropically discretized Laplacian operator at the discrete lattice point $\boldsymbol{r}$ and $\mu(\boldsymbol{r}, t)$ is the dimensionless counterpart of the Gaussian noise $\sigma(\boldsymbol{r}, t)$. Using the robustness of cell dynamical modelling and the insensitivity of results to the precise form of the local relaxation function $G_r(x)$ [2], we can replace $G_r(x)$ by the piecewise linear function

$$f_r(x)=A(\boldsymbol{r})x \qquad |x|\leq\frac{\alpha(\boldsymbol{r})}{A(\boldsymbol{r})}$$
$$=\alpha(\boldsymbol{r})\,\mathrm{sgn}(x) \qquad |x|>\frac{\alpha(\boldsymbol{r})}{A(\boldsymbol{r})}. \tag{2.15}$$

This piecewise linear function ensures a more rapid relaxation to the local fixed points, thereby enabling quicker access to the asymptotic regime. Thus, we have the required computationally efficient CDS model [5]

$$\psi(\boldsymbol{r}, t+\Delta t)=f_r(\psi(\boldsymbol{r}, t))+\frac{\Delta t}{(\Delta x)^2}\Delta_D\psi(\boldsymbol{r}, t)+\sqrt{\varepsilon}\Delta t\mu(\boldsymbol{r}, t). \tag{2.16}$$

Equation (2.16) can be written in the manifestly discrete form

$$\psi(\boldsymbol{r}, t+1)=f_r(\psi(\boldsymbol{r}, t))+D\Delta_D\psi(\boldsymbol{r}, t)+B\mu(\boldsymbol{r}, t) \tag{2.17}$$

where the time is incremented in discrete steps; $D=\Delta t/(\Delta x)^2$; and $B=\sqrt{\varepsilon}\Delta t$.

For the case with conserved order parameter, we desire to construct the CDS model which mimics the dynamics of (2.10). In the continuum case, the partial differential equation which describes the case with conserved order parameter is naively obtained by appending a $(-\nabla^2)$ operator to the chemical potential in the TDGL equation. The required CDS model for the conserved dynamics is obtained analogously [2] from (2.17) as

$$\psi(\boldsymbol{r}, t+1)=\psi(\boldsymbol{r}, t)-\Delta_D[f_r(\psi(\boldsymbol{r}, t))-\psi(\boldsymbol{r}, t)+D\Delta_D\psi(\boldsymbol{r}, t)]+B\mu(\boldsymbol{r}, t) \tag{2.18}$$

where (again) the time t is incremented in discrete steps. This is the CDS model we have used to obtain the two-dimensional results described in this paper.

There are five parameters in our model, namely, the constants $A_0(=e^{\Delta'})$ and D; the noise amplitude B; and the amplitudes of the two disorder terms $\delta a(r)$ and $\delta b(r)$. The choice of parameters is dictated by the twin requirements that (a) the scheme (2.18) be numerically stable; and (b) the results obtained be reasonable [2]. We use the parameter values $A_0 = 1.3$ and $D = 0.125$, which have proved appropriate for the case without disorder [2]. Before we proceed, some discussion of this choice of values for A_0 and D is in order. Essentially, the values of A_0 and D affect only the width of the interface between the domains and not the bulk of the domains. Asymptotically, the width of the interface (which is constant in time) is an irrelevant variable compared to the characteristic domain size (which grows in time). Thus, the only effect of the interface width is to introduce non-universal features in the scaled structure factors at early times. Asymptotically, scaled structure factors are independent of the interface width and, consequently, independent of the values of A_0 and D. This has been confirmed for the case without disorder [2] and we have also verified it for the case with disorder, though we do not present detailed results here. The asymptotic results presented below are independent of the values of A_0 and D over a broad range of values.

The choice of noise amplitude raises some important questions, in the case of segregation in pure alloys, the presence of noise only affects the smoothness of the interface between the domains. With the passage of time, the interface thickness (or raggedness) is irrelevant in comparison to the characteristic domain size. Therefore, for pure systems, noise is an irrelevant variable asymptotically and this has been also demonstrated numerically [2]. However, domain growth in disordered systems is driven by the thermally assisted hopping of energy barriers created by the disorder traps [6]. In our coarse-grained models, this probabilistic hopping is incorporated even in the deterministic models as a consequence of the probabilities in the master equation [7]. Thus, we expect that the effects of disorder and the appropriate slowing down will show up in the deterministic model also. As a matter of fact, our numerical simulations show that non-algebraic domain growth is seen in the deterministic case also. However, the deterministic case is plagued by freezing effects and it is difficult to get domain growth over extended periods of time. Thus, we choose a non-zero noise amplitude ($B = 0.3$) for our simulations. Numerically, we choose noise to be uniformly distributed between -0.3 and 0.3. (For completeness, we have also done simulations with Gaussian distributed noise. The results are identical to those presented here. Furthermore, different noise amplitudes give similar growth to those described here. We do not present these results.)

Finally, for simplicity, we choose the disorder amplitudes to be equal. The results described here are for the case where $\delta a(r)$ and $\delta b(r)$ are uniformly distributed between $-C$ and $+C$, where we will specify the different values of C subsequently. Again, for completeness, we have also performed simulations in which the disorder is Gaussian distributed. The results are identical to those presented here and, hence, we do not present the results for Gaussian distributed disorder.

3. Numerical results

We have implemented the scheme (2.18) on a 128×128 lattice with periodic boundary conditions. The quantity usually calculated is the time-dependent structure factor,

which is defined as

$$S(\boldsymbol{k}, t) = [\langle \psi(\boldsymbol{k}, t)\psi(\boldsymbol{k}, t)^* \rangle] \tag{3.1}$$

where $\psi(\boldsymbol{k}, t)$ is the Fourier transform of $\psi(\boldsymbol{r}, t)$ on the discrete lattice; the angular brackets denote an averaging over different initial conditions; the square brackets denote an averaging over different disorder configurations; and the * denotes complex conjugation. The wavevectors $\boldsymbol{k}$ take up the discrete values $2\pi(k_x, k_y)/128$, where k_x and k_y range from 1 to 128. For each fixed configuration of disorder, we obtain structure factors as averages over 20 different initial conditions. Then, we average over (typically) 20 different configurations of disorder. The time-dependent structures factors are circularly averaged to give the scalar function $S(\boldsymbol{k}, t)$, which will be shown in subsequent figures. The characteristic domain size $\langle R \rangle(t)$ is defined as the reciprocal of the first moment of the scalarized structure factor, i.e. $\langle R \rangle(t) = \langle k \rangle(t)^{-1}$, where $\langle k \rangle(t)$ is defined as

$$\langle k \rangle(t) = \frac{\int_0^{k_m} \mathrm{d}k\, kS(k, t)}{\int_0^{k_m} \mathrm{d}k\, S(k, t)} \tag{3.2}$$

where k_m is the magnitude of the largest wavevector we consider. The results presented here are for k_m equal to half the magnitude of the largest wavevector lying in the Brillouin zone of the lattice. The characteristic length scale thus measured is in units of the lattice spacing.

Before we proceed to describe our results for the conserved case, let us briefly recapitulate our numerical results [5] for the non-conserved case, i.e. the case of a random magnet. We had made two relevant observations. Firstly, the process of domain growth was characterized by a single length scale $\langle R \rangle(t)$, which had a non-algebraic temporal dependence. Our results indicated that the Huse-Henley prediction [6] ($\langle R \rangle(t) \sim (\ln t)^4$ in two dimensions) was valid over a limited range of disorder amplitudes. For higher values of disorder, slower growth was seen but this could well have been because of the freezing of domain growth at higher amplitudes of disorder. In spite of our extensive simulations, it was rather difficult to extract the domain growth law conclusively from the numerical data. Secondly, we found that the dynamical structure factor had a universal scaling form which was independent of the disorder amplitude. Our numerical results were very clear in this regard and we found that the scaled structure factors for different amplitudes of disorder coincided even in the tail region.

Let us now describe our results for segregation in a binary alloy with quenched disorder. Figure 1 shows the characteristic domain size ($\langle R \rangle(t)$) as a function of the update time t. In this figure, we have plotted $\langle R \rangle(t)^3$ versus t, as domain growth for the pure system is known to obey the Lifshitz-Slyozov growth law, $\langle R \rangle(t) \sim t^{1/3}$. In figure 1, the data for the pure system are denoted by circles and show a linear behaviour, as expected from the Lifshitz-Slyozov growth law. Domain growth for the disordered case is also shown in figure 1 and the different amplitudes of disorder are marked by the denoted symbols. For very early times, the result for the case with disorder is the same as that without disorder. This corresponds to the time regime in which the domains are small so that the growth is unaffected by the disorder. However, there is a rapid crossover to a regime in which the growth is different from that of the pure case. The onset of this crossover is earlier for larger amplitudes of disorder. We have attempted to fit the domain growth for the disordered case to a power law form as $\langle R \rangle(t) \sim t^{\phi}$. However, it is not possible to fit the domain growth to a power law form over extended

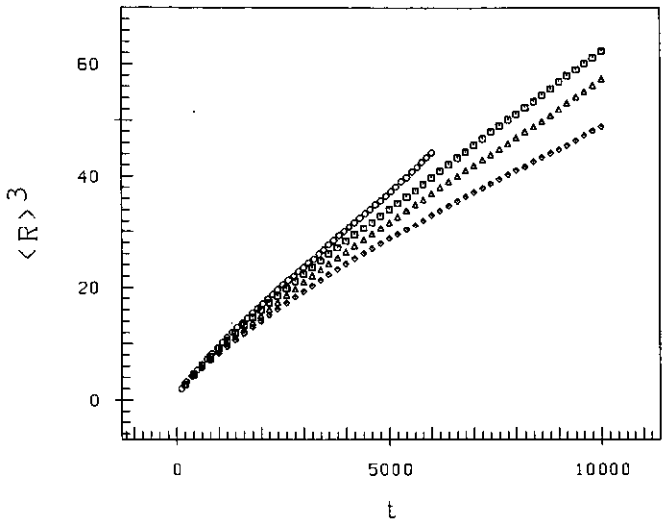

Figure 1. Plot of $\langle R\rangle(t)^3$ versus t (where $\langle R\rangle(t)$ is the characteristic length scale at update time t) for the pure case (marked by circles) and the disordered case with disorder amplitudes $C = 0.3$ (□), 0.4 (△), 0.5 (◇).

periods of time. Thus, we believe that the domain growth for the disordered binary alloy is non-algebraic.

As we remarked earlier, the generic growth law for growth that is governed by barrier hopping is expected to be of the form $\langle R\rangle(t) \sim (\ln t)^x$, where x is the growth exponent. Figure 2 shows the effective exponent x versus $100/t$ for the data from figure 1 (excluding, of course, the data for the pure case). An estimate of the effective exponent

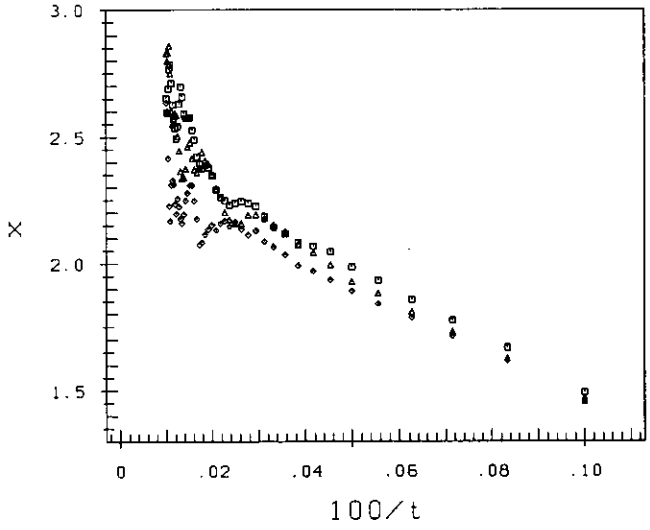

Figure 2. Plot of effective exponent x versus $100/t$. The effective exponent is the instantaneous slope of the plot $\ln(\langle R\rangle(t))$ versus $\ln(\ln t)$ for the results with non-zero disorder from figure 1. The different disorder amplitudes are denoted by the same symbols as in figure 1.

is obtained as the effective slope of the curve obtained by plotting $\ln(\langle R\rangle(t))$ versus $\ln(\ln t)$. The asymptotic value of the effective exponent should give the true value of the exponent. However, it is clear from figure 2 that the effective exponent shows a systematic upward trend and does not saturate out within the maximum time of our simulation, namely 10 000 updates. To demonstrate the difficulty of extracting the asymptotic exponent, figures 3(*a*) and 3(*b*) plot, respectively, $\langle R\rangle(t)$ versus $(\ln t)^{5/2}$ and $\langle R\rangle(t)$ versus $(\ln t)^3$ for the data from figure 1. Figure 3(*a*) demonstrates that the higher values of disorder are described well by the domain growth law $\langle R\rangle(t) \sim (\ln t)^{5/2}$. However, figure 3(*b*) indicates that the appropriate domain growth law for lower disorder amplitudes is more like $\langle R\rangle(t) \sim (\ln t)^3$. Thus our numerical results are not conclusive in this regard. At most, we can only say that the form $\langle R\rangle(t) \sim (\ln t)^x$ (with x increasing with decreasing disorder amplitude) provides a reasonable fit to our numerical data. Of course, it is possible that our simulations are not yet in the asymptotic regime. As a matter of fact, the Huse–Henley argument [6] relates the growth exponent x to two static exponents, namely the roughening exponent and the pinning energy exponent. Thus, the asymptotic growth exponent should not depend upon whether the order parameter is non-conserved or conserved. However, we do not see the growth law $\langle R\rangle(t) \sim (\ln t)^4$ in our simulations for the disordered binary alloy.

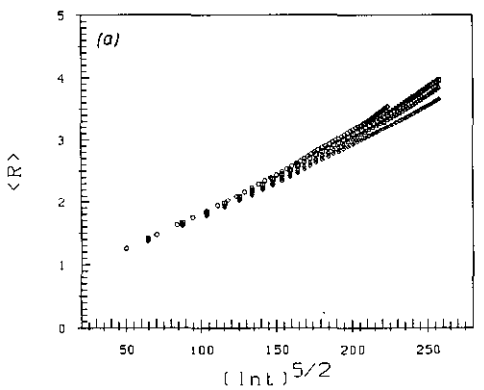

Figure 3(*a*). Plot of $\langle R\rangle(t)$ versus $(\ln t)^{5/2}$ for the data from figure 1. We use the same symbols as in figure 1 to denote the different disorder amplitudes.

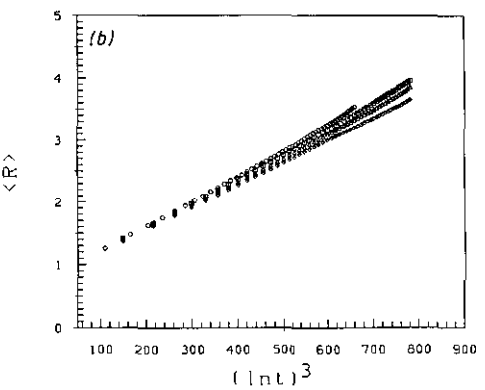

Figure 3(*b*). Plot of $\langle R\rangle(t)$ versus $(\ln t)^3$ for the data from figure 1. Again, we use the same symbols as in figure 1 to denote the different disorder amplitudes.

We have also performed simulations for disorder amplitudes which are both smaller and larger than those shown here. For smaller values of disorder, the domain growth is indistinguishable from the pure system for all times before the finite size effects become important. This is because the noise amplitudes are large enough that the disorder barriers do not act as an obstacle to domain growth over the time-scale of observation. For disorder values larger than those shown in the figures, domains freeze into metastable states too soon and do not enable us to observe an extended period of domain growth. Clearly, at lower noise amplitudes, one could see non-algebraic growth effects at smaller disorder amplitudes than those shown here. However, at the same time, the disorder amplitudes at which freezing effects plague our simulations are also reduced. Thus, there is a narrow window of disorder amplitudes (dependent on the noise amplitude) in which we can observe non-algebraic domain growth over an extended period of time.

Finally, we consider the scaled structure factors. We have confirmed (not shown here) that the scaled structure factor for each value of disorder shows dynamical scaling over extended periods of time. Figure 4(a) is a plot of $S(k, t)\langle k\rangle(t)^2$ versus $k/\langle k\rangle(t)$ for data from different disorder amplitudes (denoted by the symbols shown). It is clear from figure 4(a) that the universal structure factors for different disorder amplitudes are the same as that for the pure system case. Figure 4(b) plots $\ln(S(k, t)\langle k\rangle(t)^2)$ versus $k/\langle k\rangle(t)$ for data from figure 4(a), so as to clarify the tail structure. The coincidence of the universal structure factors is seen to extend even to the tail region. We have seen a similar super-universality for the case with non-conserved order parameter [5]. It is a consequence of the fact that the structure factor is the statistical property of a set of sharp, random interfaces and is independent of the fashion in which these interfaces are obtained.

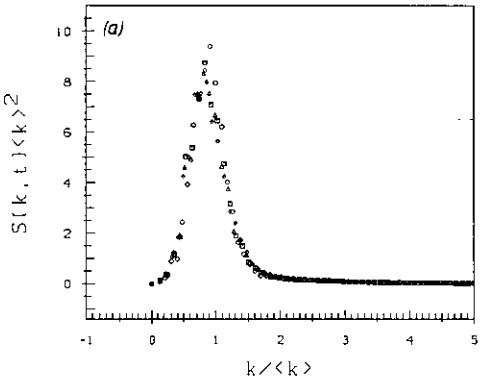

Figure 4(a). Plot of the scaled structure factors $S(k, t)\langle k\rangle(t)^2$ versus $k/\langle k\rangle(t)$ for the pure case at time $t = 6000$ (marked by circles); and for the disordered case with disorder amplitudes $C = 0.3, 0.4, 0.5$ all at time $t = 10\,000$ (symbols as in figure 1). The structure factors are obtained as statistical averages over runs from 20 different initial conditions for each of 20 different disorder configurations.

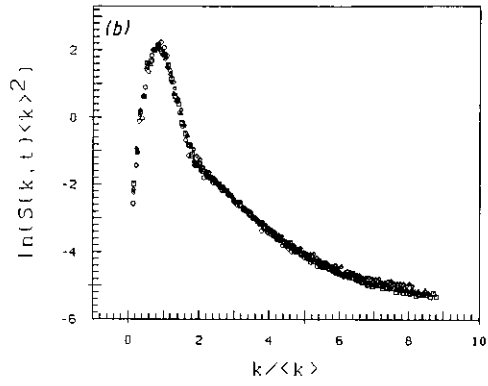

Figure 4(b). Semi-logarithmic plot of the scaled structure factors from figure 4(a), i.e. plot of $\ln(S(k, t)\langle k\rangle(t)^2)$ versus $k/\langle k\rangle(t)$. The symbol used are the same as in figure 4(a).

4. Summary and discussion

In this paper we have presented detailed numerical results from a cell dynamical system (CDS) study [2] of domain growth in binary alloys with quenched disorder. We started off from a coarse-grained Hamiltonian which incorporates the effects of quenched disorder by assigning a spatial dependence to the coefficients of the various order parameter-dependent terms. This Hamiltonian can be used to describe the dynamics of magnets with quenched disorder (via a TDGL equation) and the dynamics of binary alloys with quenched disorder (via a generalization of the Cahn-Hillard-Cook equation). We did not integrate the resulting partial differential equation directly but rather used a computationally efficient CDS model which was equivalent to the partial differential equation. The enhanced numerical efficiency enabled us to perform extensive simulations of the effects of quenched disorder on domain growth in binary alloys.

Our numerical results consisted of two important observations. Firstly, we were able to establish the existence of a unique length scale that characterizes domain growth, even in disordered binary alloys. We were also able to confirm that this characteristic length scale did not have an algebraic dependence on time. We then attempted to fit it to a law of the type $\langle R\rangle(t) \sim (\ln t)^x$ (motivated by theoretical considerations) but our numerical results were (at best) able to extract an effective exponent which increases from $\frac{5}{2}$ to 3 with decreasing disorder amplitude. It is possible that the asymptotic growth law is actually $\langle R\rangle(t) \sim (\ln t)^4$ for all amplitudes of disorder (as predicted in the non-conserved case [6]) but our numerical results did not access a time regime in which this was true. Secondly, we were able to clearly demonstrate numerically that the scaled structure factor was independent of the value of disorder and was actually the same as that in the pure case. We had earlier demonstrated this to be true in the non-conserved case also [5].

The results presented here are part of a larger project to investigate the effects of quenched disorders on domain growth using coarse-grained CDS models. Previous studies have consisted of Monte Carlo simulations and have not been able to make quantitative predictions (with one exception [13]) regarding the nature of the domain growth law and the super-universality of the scaled structure factors. We have also completed a study of ordering and phase segregation kinetics in the presence of quenched random fields and will present these results elsewhere [14]. It is our belief that, as in the pure case, coarse-grained models will be considerably more successful than Monte Carlo models in elucidating the nature of domain growth in disordered systems.

Acknowledgments

The authors are grateful to D Chowdhury, with whom they collaborated on the earlier part of this project. They are also grateful to him for many useful discussions and for a critical reading of this manuscript. SP is grateful to A Bray for a number of insightful comments and for communicating his results for the non-conserved case prior to publication. SP is also grateful to K Binder for his warm hospitality at Mainz, where some of the numerical computations described in the text were performed. This work was supported, in part, by the DFG (Germany) under SFB 262.

References

[1] For reviews, see:
Gunton J D, San Miguel M and Sahni P S 1983 *Phase Transitions and Critical Phenomena* vol 8, ed C Domb and J L Lebowitz (New York: Academic) p 267
Binder K 1987 *Rep. Prog. Phys.* **50** 783
Furukawa H 1985 *Adv. Phys.* **34** 703
Komura S 1988 *Phase Transitions* **12** 3; 1988 *Dynamics of Ordering Process in Condensed Matter* ed S Komura and H Furukawa (New York: Plenum)
Grant M *Int. J. Mod. Phys.* B in press
[2] Oono Y and Puri S 1987 *Phys. Rev. Lett.* **58** 836; 1988 *Phys. Rev.* A **38** 434
Puri S 1988 *Phys. Lett.* **134A** 205
Puri S and Oono Y 1988 *J. Phys. A: Math. Gen.* **21** L755; 1988 *Phys. Rev.* A **38** 1542
[3] Puri S and Dunweg B 1992 in press

[4] (*a*) For Monte Carlo studies of the non-conserved case with quenched disorder, see:
Grest G S and Srolovitz D J 1985 *Phys. Rev.* B **32** 3014
Chowdhury D, Grant M and Gunton J D 1987 *Phys. Rev.* B **35** 6792
Chowdhury D and Kumar S 1987 *J. Stat. Phys.* **49** 855
Oh J H and Choi D I 1986 *Phys. Rev.* B **33** 3448
Chowdhury D 1990 *J. Physique* **51** 2681
Bray A J and Humayun K 1991 *J. Phys. A: Math. Gen.* **24** L1185
(*b*) For Monte Carlo studies of the non-conserved case with annealed disorder, see:
Srolovitz D J and Hassold G N 1987 *Phys. Rev.* B **35** 6902
Mouritsen O G and Shah P J 1989 *Phys. Rev.* B **40** 11445
[5] Puri S, Chowdhury D and Parekh N 1991 *J. Phys. A: Math. Gen.* **24** L1087
[6] Huse D A and Henley C L 1985 *Phys. Rev. Lett.* **54** 2708
[7] Binder K 1974 *Z. Phys.* **267** 313
[8] Hohenberg P C and Halperin B I 1977 *Rev. Mod. Phys.* **49** 435
[9] Grinstein G, Ma S K and Mazenko G F 1977 *Phys. Rev.* B **15** 258
Ma S K 1982 *Modern Theory of Critical Phenomena* (Reading, MA: Addison-Wesley)
[10] Puri S unpublished
[11] Cahn J W and Hilliard J E 1958 *J. Chem. Phys.* **28** 258; 1959 *J. Chem. Phys.* **31** 688
Cahn J W 1969 *Acta. Met.* **9** 795
Cook H E 1970 *Acta. Met.* **18** 297
[12] Parekh N and Puri S 1990 *J. Phys. A: Math. Gen.* **23** L1085
[13] Bray A J and Humayun K 1991 *J. Phys. A: Math. Gen.* **24** L1185
[14] Puri S 1992 in press